nature chemistry

Article

https://doi.org/10.1038/s41557-024-01455-7

A catalytic process enables efficient and programmable access to precisely altered indole alkaloid scaffolds

Received: 5 February 2023

Accepted: 18 January 2024

Published online: 19 February 2024

Check for updates

Youming Huang[1,2,6], Xinghan Li[1,2,6], Binh Khanh Mai[3,6], Emily J. Tonogai[4], Amanda J. Smith[4], Paul J. Hergenrother[4,5] ✉, Peng Liu[3] ✉ & Amir H. Hoveyda[1,2] ✉

A compound's overall contour impacts its ability to elicit biological response, rendering access to distinctly shaped molecules desirable. A natural product's framework can be modified, but only if it is abundant and contains suitably modifiable functional groups. Here we introduce a programmable strategy for concise synthesis of precisely altered scaffolds of scarce bridged polycyclic alkaloids. Central to our approach is a scalable catalytic multi-component process that delivers diastereo- and enantiomerically enriched tertiary homoallylic alcohols bearing differentiable alkenyl moieties. We used one product to launch progressively divergent syntheses of a naturally occurring alkaloid and its precisely expanded, contracted and/or distorted framework analogues (average number of steps/scaffold of seven). In vitro testing showed that a skeleton expanded by one methylene in two regions is cytotoxic against four types of cancer cell line. Mechanistic and computational studies offer an account for several unanticipated selectivity trends.

Lead discovery is expedited when distinct compound arrays can be evaluated, placing the burden on the art of small molecule synthesis (molecular weight ≤1,000 g mol^{-1})[1]. Based on the premise that an even mildly bioactive natural product (NP) may be viewed as a pre-validated starting point[2], methods[3] have been introduced for their functional group and/or stereochemical alterations. These strategies are applicable, however, if a NP is available in sufficient quantities and contains a suitably reactive functional group[4]. In contrast, schemes designed for making precisely altered scaffolds accessible are uncommon[5], and those that are available typically generate analogues that contain multiple modifications (stereochemical, functional and constitutional). In this Article, we present a strategy to address this shortcoming for a key class of bioactive NPs.

The principal aim of these investigations was to find ways of efficiently synthesising skeletally diverse indole alkaloids (Fig. 1a). Related collections have been prepared, but the analogues were either differentiated by multiple changes, most stereochemical or functional group variations[6], or were also marked by peripheral and constitutional (bond connectivity) adjustments[7]. We had several reasons to concentrate on these compounds. These were as follows: (1) the bridged bicyclic amine scaffold can be found in myriad NPs[8]. While some display different types of bioactivity (for example, pericine is an analgesic/cytotoxic agent and (+)-16-hydroxy-16,22-dihydroapparicine[9] is anti-malarial[10]), little is known about others (such as curan[11] and isobrafuedin[12]). (2) Many indole alkaloids can be obtained in only minute amounts, making their laboratory synthesis imperative. (3) Most alkaloid frameworks are devoid of a functional group that can be used for scaffold alteration, especially if the modifications are not to alter stereochemistrical identity. One possibility is oxidative

[1]Supramolecular Science and Engineering Institute, University of Strasbourg, CNRS, Strasbourg, France. [2]Department of Chemistry, Merkert Chemistry Center, Boston College, Chestnut Hill, MA, USA. [3]Department of Chemistry, University of Pittsburgh, Pittsburgh, PA, USA. [4]Department of Chemistry, Carl Woese Institute for Genomic Biology, University of Illinois, Urbana, IL, USA. [5]Cancer Center at Illinois, University of Illinois, Urbana, IL, USA. [6]These authors contributed equally: Youming Huang, Xinghan Li. ✉e-mail: hergenro@illinois.edu; pengliu@pitt.edu; amir.hoveyda@bc.edu

https://doi.org/10.1038/s41557-024-01455-7

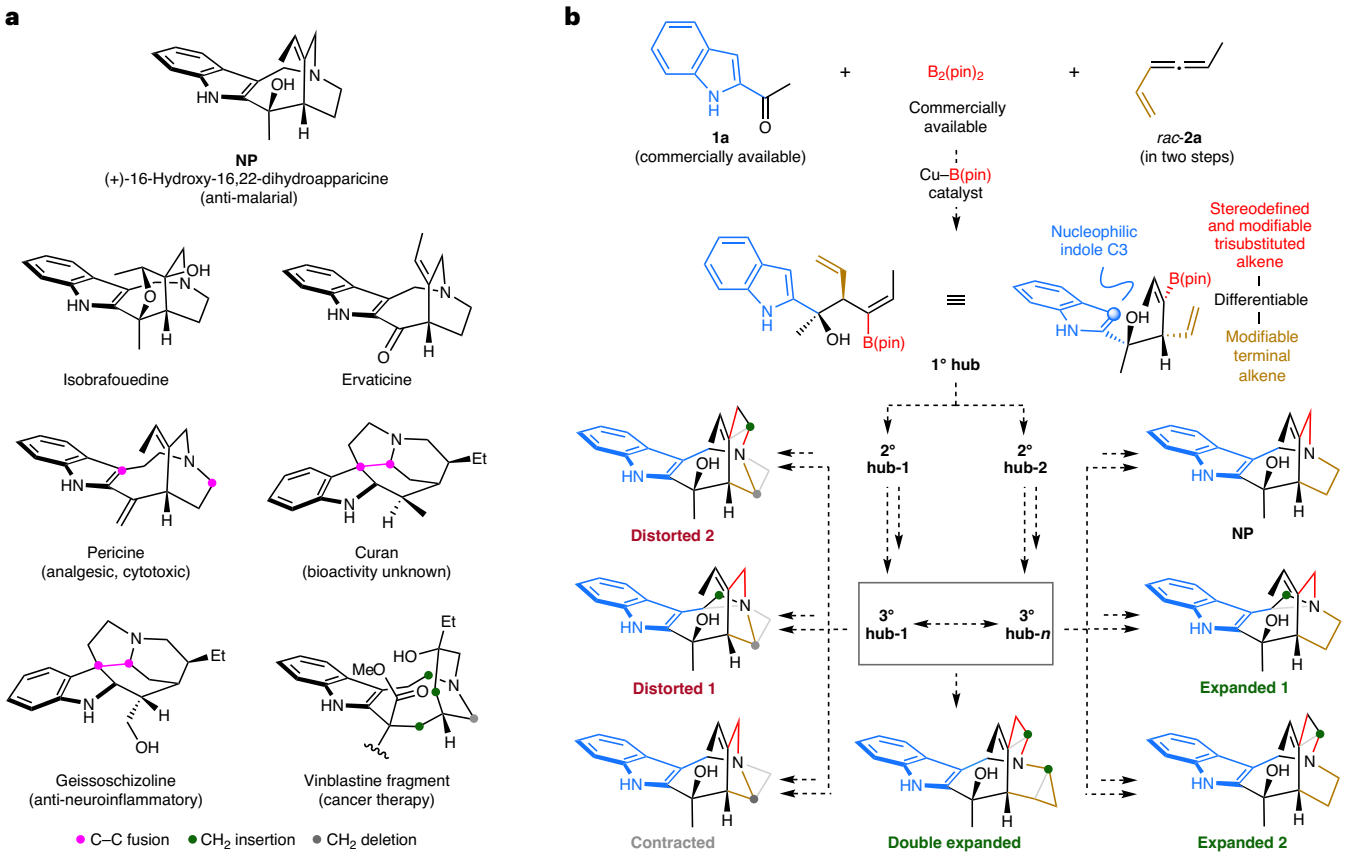

Fig. 1 | Bridged polycyclic indole alkaloids, the foundational multi-component process and its applicability. a, Alkaloids are large in number and exhibit different types of bioactivity. Consequently, analogues such as those of 16-hydroxy-16,22-dihydroapparicine arising from one- or two-methylene expansion, contraction or both (distortion), would be of interest. This is evident by a comparison with fragments found in related compounds with established therapeutic capabilities, such as vinblastine, showing that these scaffolds are linked by a combination of methylene unit expansion and/or contraction at different regions of their skeletons. As these NPs are available in only minute amounts and lack an easily modifiable site, late-stage framework editing strategies are not applicable. **b**, A multi-component catalytic diastereo- and enantioselective process would generate a densely functionalized product, or a primary hub (**1° hub**), containing readily alterable and differentiable mono-substituted olefin and a stereochemically defined trisubstituted alkenyl boronate. Progressively divergent conversion to **2° hubs** and a larger number of **3° hubs** can lead to precisely modified expanded, contracted or distorted frameworks (green dot denotes an added methylene and grey dot denotes a deleted methylene). The existing diastereo- and enantioselective protocols, catalysed by a copper complex and involving ketones, generate multifunctional homoallylic alcohols, but versatility can still be greater if the allylic substituent were to be more easily alterable and the alkenyl moiety were to have stereochemical identity. pin, pinacolato.

cleavage of the trisubstituted alkene followed by a Baeyer–Villiger reaction to generate a ring-expanded lactone. However, as we would later confirm, amines preclude the use of oxidative procedures. Further, our intent was to implement skeletal modification without incorporating additional polar groups. We favoured skeletal variants arising through precise insertion and/or deletion of one or more methylene units. Late-stage editing is unrealistic because of the latter factors (2 and 3). (4) There is structural diversity among indole alkaloid NPs. Several, represented by geissoschizoline (Fig. 1a), a candidate for treating Alzheimer's disease[13], feature a transannular linkage within their polycyclic structure. Whereas most contain an *E*-trisubstituted alkene, some have a *Z* isomer (for example, ervaticine; Fig. 1a)[14]. (5) There are unexplored gaps in the NP frameworks. Expansion and/or contraction of different scaffold regions by one or more methylene units leads to distorted analogues, one being a fragment of vinblastine (Fig. 1a), a cancer chemotherapy agent. We concluded that there are probably undiscovered frameworks that could be an asset to drug discovery[15].

We chose to focus on 16-hydroxy-16,22-dihydroapparicine (**NP**; Fig. 1a), a comparatively simple structure. Our decision was founded on the principle that complexity should be based on more than solely the intricacy of a single molecule or less than a handful of NPs. Rather, it should also be defined by the number and diversity of the targeted collection as well as the efficiency, precision and selectivity with which it is assembled. The only reported enantioselective synthesis of **NP** consists of a longest linear sequence (LLS) of 23 steps[16]. The route can be used to access serviceable quantities of the molecule (5% overall yield). Nevertheless, the sequence lacks a suitable diversification point and therefore does not lend itself to efficient preparation of precisely altered scaffolds. For each skeletal variant a new scheme would have to be re-negotiated.

Our idea was that a multifunctional homoallylic tertiary alcohol would be an attractive point of origin or a primary hub (**1° hub**; Fig. 1b). This densely packed fragment could be obtained through a catalytic diastereo- and enantioselective process involving an indole-substituted ketone (**1a**), bis(pinacolato)diboron ($B_2(pin)_2$) and a vinylallene (*rac*-**2a**). With a vinyl group at the allylic position and a stereochemically defined trisubstituted alkenyl–B(pin) moiety, both modifiable and differentiable, together with indole's mildly nucleophilic C3, it would be possible to convert **1° hub** to several **2° hubs**. The latter compounds would in turn be transformed to an expanded suite of specifically outfitted **3° hubs**, precursors to precisely remodelled scaffolds. Through a network of overlapping pathways, minimizing step-count and obviating complete route repetition, **NP** and various skeletal analogues would

https://doi.org/10.1038/s41557-024-01455-7

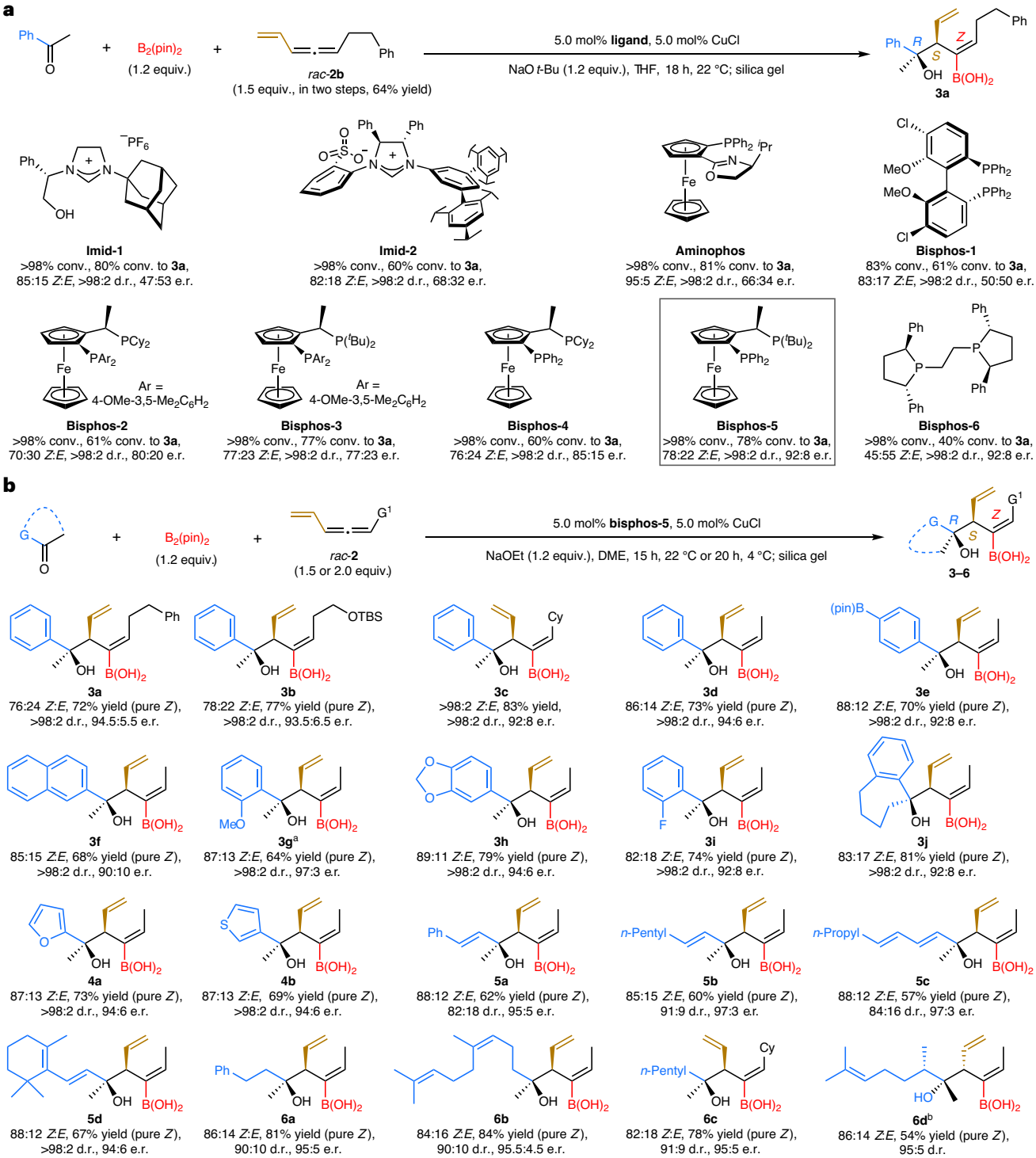

Fig. 2 | Catalyst screening and the scope of the multi-component process. **a**, Screening of different types of chiral ligand began with the copper complex of N-heterocyclic carbene derived from **imid-1**, which had formerly been found to be the most effective in 1,6-conjugate additions involving the same type of allenes, $B_2(pin)_2$ and acyclic dienoates; this reaction, while efficient and diastereoselective, was barely enantioselective. Similar results were obtained with other N-heterocyclic carbene ligands, aminophosphine with a P and N ligation site, as well as biaryl bisphosphines. Enantioselectivities improved with ferrocene-based bisphosphines, with **bisphos-5** (in box) delivering the highest e.r. Ethyl-bridged **bisphos-6** was as enantioselective as **bisphos-5** but gave a lower ratio of *E*:*Z* isomer (readily separable). **b**, The catalytic multi-component process has considerable scope, in a single step generating densely functionalized fragments that contain chemoselectively alterable vinyl (in brown) and trisubstituted alkenyl–B(pin) (in red). A range of ketone substituents (in blue) is tolerated, including aryl moieties that are electron-deficient (**3e**) or electron-rich (**3g**–**3h**), heteroaryl groups (**4a** and **4b**), alkenyl units (**5a**–**5d**) and alkyl moieties (**6a**–**6d**). In all instances, the trisubstituted alkenyl isomers are readily separable; the yields shown are for the pure *Z* isomers. Reactions were performed under N_2 atmosphere. Conversion to product (>98% in all cases), *Z*:*E* ratio and d.r. were measured by analysis of 400 MHz ^{1}H nuclear magnetic resonance spectra of unpurified mixtures with diphenylmethane serving as the internal standard (±2%). Yield of purified product, averaged over at least three runs (±5%) of enantioselectivities, was determined by high-performance liquid chromatography analysis (±1%). [a]With **bisphos-3**; 59:41 e.r. with **bisphos-5**. [b]With *ent*-**bisphos-5**; 39% yield, 80:20 d.r. with **bisphos-5**. See Supplementary Section 4 for details. THF, tetrahydrofuran; Ar, aryl group; TBS, *tert*-butyldimethylsilyl; DME, dimethoxyethane.

be secured (**expanded 1**, **expanded 2**, **double expanded**, **contracted**, **distorted 1** and **distorted 2**).

Two other considerations merit mention: (1) we were aware that our plans might challenge the state of the art in chemical synthesis and that new methods, other than the foundational catalytic process, might be needed. We considered this a positive attribute. (2) Vis-à-vis diversification, the proposed strategy represents a blend of two existing approaches: diversity-oriented synthesis (DOS)[17–19] and diverted total synthesis (DTS)[20]. One type of DOS is centred on a core platform. In DTS, one or more intermediates, generated en route to the target molecule, might serve as branching points for implementing functional and/or stereochemical variations that may be accompanied by framework alterations caused by multiple connectivity changes[21,22]. Analogous to DTS but unlike DOS, in our approach, a NP would serve as the parent skeleton. Neither DOS nor DTS has been used to implement precise scaffold alterations.

Results and discussion

A suitable catalytic multi-component process

There has been ample progress in the development of catalytic multi-component processes involving ketones[23]. This includes transformations that are promoted by a Cu–B(pin) or a Cu–H complex and involve mono-substituted allenes[24,25], enynes[26] and dienes[27–29] as organocopper precursors. However, none of the reactions affords products amenable to efficient alkaloid synthesis. Furthermore, we were far from confident about identifying conditions for the proposed multi-component process to proceed efficiently or diastereo- and/or enantioselectively. The 1,3-disubstituted allenes are chiral, raising the question of whether they must be used in the enantiomerically enriched form. The only reported case pertains to 1,6-conjugate additions to α,β,γ,δ-unsaturated diesters, promoted by a N-heterocyclic carbene–copper complex[30], where a vinylallene's enantiomeric purity turned out to be inconsequential. Mechanistic studies revealed that the Cu–allyl species derived from regioselective addition of the Cu–B(pin) complex undergoes π-allyl isomerization, engendering rapid loss of stereochemical identity. Besides, high selectivity was shown to be linked to a substrate's 1,3-dicarbonyl moiety, which, according to density functional theory (DFT) studies, coordinates with the available alkali metal salt to enhance transition state organization. We also knew that with ketones, based on precedent[24], high regio- and stereochemical control would be difficult to achieve. Making matters still dicier, the published method was found to be confined to aryl ketones[24]; additions to the less reactive aliphatic variants suffered from adventitious enolate formation.

We first evaluated the reaction of acetophenone with *rac*-**2b** (synthesized in two steps and 64% yield; Fig. 2a), and $B_2(pin)_2$ (commercially available) with the catalyst earlier found to be effective for the aforementioned 1,6-conjugate additions[30]. This was the copper complex generated from **imid-1**. The transformation proceeded to completion, affording **3a** in 85:15 *Z*:*E* and >98:2 diastereomeric ratio (d.r.), but enantioselectivity was nominal (47:53 enantiomeric ratio (e.r.)). Related complexes, such as that originating from **imid-2**, were slightly more discriminating (68:32 compared with 47:53 e.r.), and those generated from P,N-type ligands, such as **aminophos**, were only more *Z*-selective. With **bisphos-1**, optimal for the reactions between ketones and mono-substituted allenes[24], **3a** was generated in 83:17 *Z*:*E* and >98:2 d.r., albeit racemically. Reactions with **bisphos-2**–**bisphos-5**, which contain a triarylphosphine moiety, afforded **3a** with similar *Z* selectivity and d.r. Notably, the **bisphos-5**–Cu-catalysed process afforded **3a** in 92:8 e.r. (for determination of stereochemical identity, see Fig. 3a). With **bisphos-6**, the transformation was equally efficient and enantioselective, but the *Z*:*E* ratio was lower (see Fig. 3b and the related discussion regarding this finding).

By using **bisphos-5**, we synthesized an assortment of homoallylic tertiary alcohols (Fig. 2b), including those derived from aryl (**3a**–**3j**), heteroaryl (**4a** and **4b**), alkenyl (**5a**–**5d**) and alkyl ketones (**6a**–**6d**), which were formed in 90:10–97:3 e.r.; *Z*:*E* selectivities varied from 76:24 to 89:11 with one curious exception. Reaction of cyclohexyl-substituted vinylallene afforded **3c** only as the *Z* isomer, whereas the *Z*:*E* ratio for the same allene with *n*-hexyl-substituted ketone to afford **6c** was in the expected range (82:18 *Z*:*E*; see Fig. 6 and the corresponding discussion for further analysis). The alkenyl isomers were separable by silica gel chromatography, and the trisubstituted alkenyl boronic acids were isolated as pure *Z* isomers (>98%, 54–84% yield).

Reactions of the more sizeable aryl and heteroaryl group ketones afforded homoallylic alcohols in >98:2 d.r. Whereas d.r. was lower with alkenyl (**5a**–**5c**) and aliphatic ketones (**6a**–**6c**), diastereoselectivity was complete with a bulkier enone (**5d**). With *ent*-**bisphos-5**, we obtained **6d** in 54% yield (pure *Z* isomer) and 95:5 d.r.; this represented the matched catalyst–substrate pairing, as with **bisphos-5**, the transformation was lower yielding and less stereoselective (80% versus >98% disappearance of the ketone (conv.), 39% yield (pure *Z*), 80:20 d.r.).

Two additional points are worth noting: (1) contrary to most instances when **bisphos-5** was optimal, the reaction affording *ortho*-methoxyphenyl-substituted **3g** was scarcely enantioselective (59:41 e.r.; 81% yield (pure *Z*), >98:2 d.r.). Further screening indicated that, remarkably, **bisphos-3** is superior in this case: **3g** was formed with far higher enantioselectivity (97:3 e.r.; 64% yield (pure *Z*), >98:2 d.r.; see Fig. 6 and the related discussion for further analysis). Reaction with *ortho*-fluorophenyl ketone afforded **3i** and **3j** in 92:8 e.r. when **bisphos-5** was used. (2) Transformations involving the smaller methyl-substituted vinylallene (compared with **2b**), relevant to the planned indole alkaloids syntheses, were efficient and selective. Conversion of the C–B bond to a C–H bond was high yielding (see Supplementary Section 5.1 for details); for example, the disubstituted alkene derived from **3d** was isolated in 82% yield (pure *Z*). Functionalization at the alkenyl–$B(OH)_2$ site, generating C–aryl, C–alkenyl or C–alkyl bonds, proceeded stereoretentively(see Supplementary Section 5.2 for details). One example is the conversion of **3d** to allylic alcohol **7a** (Fig. 3a)[31], the precursor to **7b**, the X-ray structure of which confirmed the stereochemical identity of the products(see Supplementary Section 4.2 for details).

Preparation of 1° hubs

To synthesize the **1° hub** (Fig. 1b), we examined the reaction of 2-indolyl ketone **1a** (purchasable), $B_2(pin)_2$ (purchasable) and vinylallene *rac*-**2a** (prepared in two steps, 50% yield) under the foregoing conditions (**bisphos-5**). There was no conversion after 30 h, leading us to suspect that the indole NH might cause catalyst inhibition. We therefore switched to N-benzyl-protected derivative **1b** (Fig. 3b; prepared in one step and 77% yield), which reacted efficiently and with complete diastereoselectivity. To our surprise and disconcertment, however, the **1° hub** was formed in 53:47 e.r. Re-examination of alternative ligands (Fig. 2a) led us to identify a solution in the form of using **bisphos-2**. That is, the catalyst that promoted addition to acetophenone in only 80:20 e.r. (Fig. 2a), was, in this particular case, the most effective. These findings underscore the view, articulated two decades ago[32], that generality arises from diversity. That is, the most effective catalyst in a particular case can be different from what is marked as 'optimal' based on methodological studies, pointing to the importance of the availability of a collection of catalyst candidates—the same diversity-based logic being applied to drug lead discovery.

We isolated **1° hub** in 80% yield, >98:2 *Z*:*E* ratio, >98:2 d.r. and 95:5 e.r., along with the easily separable *E*-isomer (**1° hub(*E*)**) in 18% yield, >98:2 *E*:*Z* ratio, >98:2 d.r. and 88:12 e.r. Oddly, the latter two compounds were generated with the opposite sense of enantioselectivity compared with the other ketone substrates (Figs. 2 and 3a). This was equally unanticipated, as we did not suspect a stereochemical reversal until alarmed by the results of DFT studies (see Fig. 6 and the associated discussion). The stereochemical identity of **1° hub** was verified by the

https://doi.org/10.1038/s41557-024-01455-7

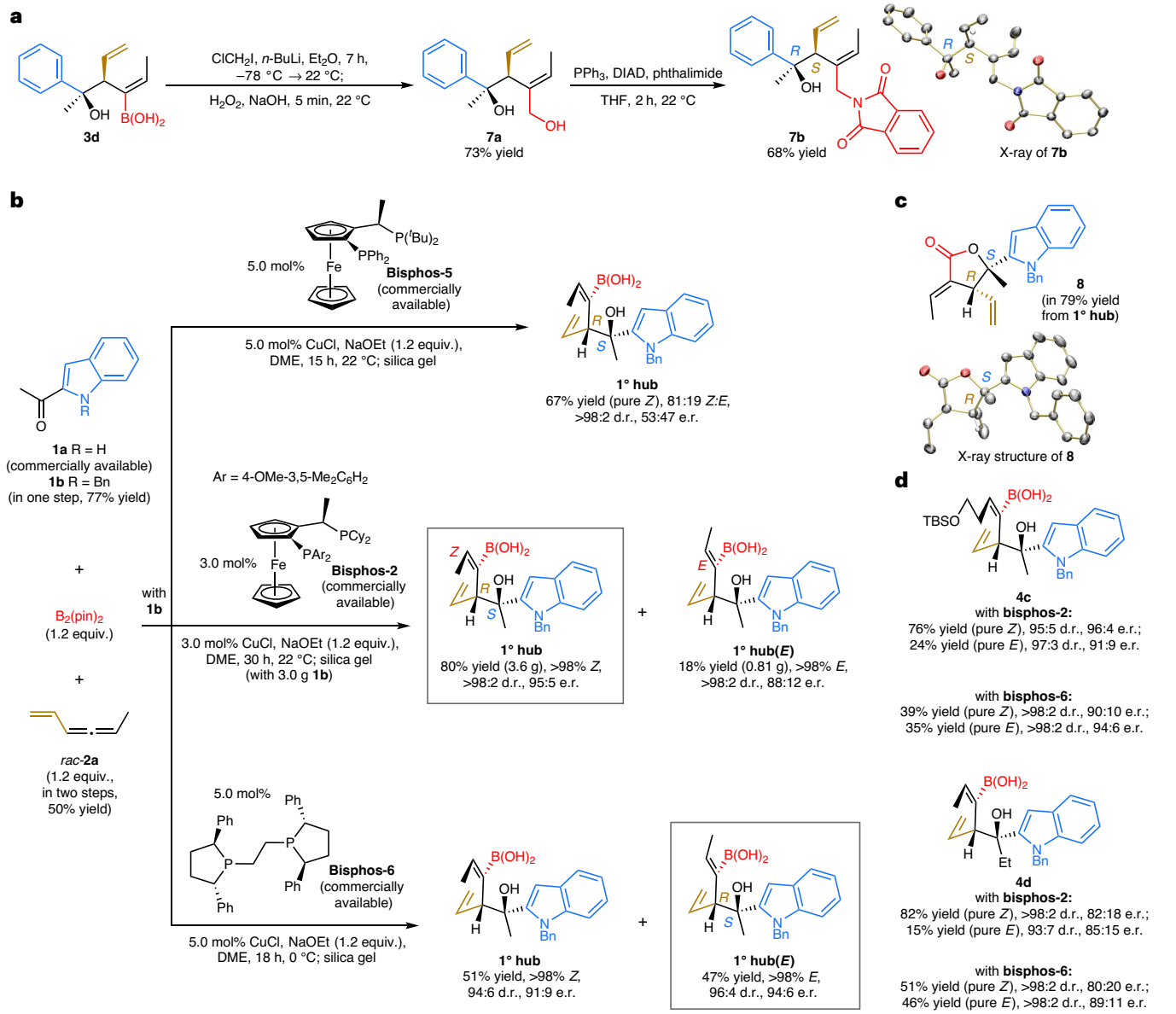

Fig. 3 | Diastereo- and enantioselective synthesis of the primary hub and some surprising observations along the way. a, The absolute stereochemistry of products of the type in Fig. 2, which bear three key exchangeable/modifiable moieties (aryl/heteroaryl in blue, alkenyl boronate in red and vinyl unit in brown), was established by X-ray crystallography. **b**, Surprisingly, the chiral catalyst derived from **bisphos-5**, optimal for most other ketones (Fig. 2b), was found to be minimally enantioselective when indolyl ketone **1b** was the substrate. Further screening revealed that the most effective catalyst to generate the envisioned **1° hub** is the copper complex derived from **bisphos-2**, namely the complex that was found in the original screening studies to afford **3a** in just 80:20 e.r. **c**, Equally surprising, as initially predicted by DFT studies and later substantiated by X-ray crystallography, the reactions with indolyl ketone **1b** proceeded with the opposite sense of enantioselectivity (for mechanistic studies, see Fig. 6). **d**, Products derived from other vinylallenes and ketones may be used to generate functionally, as well as skeletally altered analogues. DIAD, diisopropylazadicarboxylate; Bn, benzyl. See Supplementary Sections 4.2 and 6 for details.

X-ray structure of lactone **8** (Fig. 3c), confirming the validity of the DFT prediction (see Supplementary Section 6.2 for further details). A more efficient way of obtaining **1° hub(*E*)**, relevant to preparation of ***Z*-NP** and the related skeletally modified analogues, would be with the less *Z*-selective **bisphos-6**. Under these latter conditions, **1° hub(*E*)** was formed in 47% yield and 94:6 e.r.

The reactions are scalable: 3.0 g of **1b** was converted to 3.6 g of **1° hub** and 0.81 g of **1° hub(*E*)**. Transformations of **1b** with other allenes were similarly efficient and selective, as exemplified by silyl ether **4c** (Fig. 3d). Additions to ketones with less differentiable substituents were less enantioselective (**4d**). Such compounds may be viewed as alternative primary hubs that can be transformed to modified frameworks that contain peripheral/stereochemical alterations, or be made suitable for covalent ligation to another entity.

Divergent syntheses of 2° and 3° hubs

We converted **1° hub** to **2° hub-1** and **2° hub-2** (Fig. 4a), featuring a one- and a two-methylene extension at the alkenyl boronic acid site, respectively. This was accomplished by single[31] and double[33] Matteson homologation, respectively, followed by oxidation (80% and 61% yield, respectively). As the first tertiary hub, we opted for a structure that, other than the missing indolyl linkage, was identical to **NP**. Conversion of **2° hub-1** to **3° hub-1** was effected in five steps (43% yield). After silyl ether formation, the compound was treated with zirconocene chloride

https://doi.org/10.1038/s41557-024-01455-7

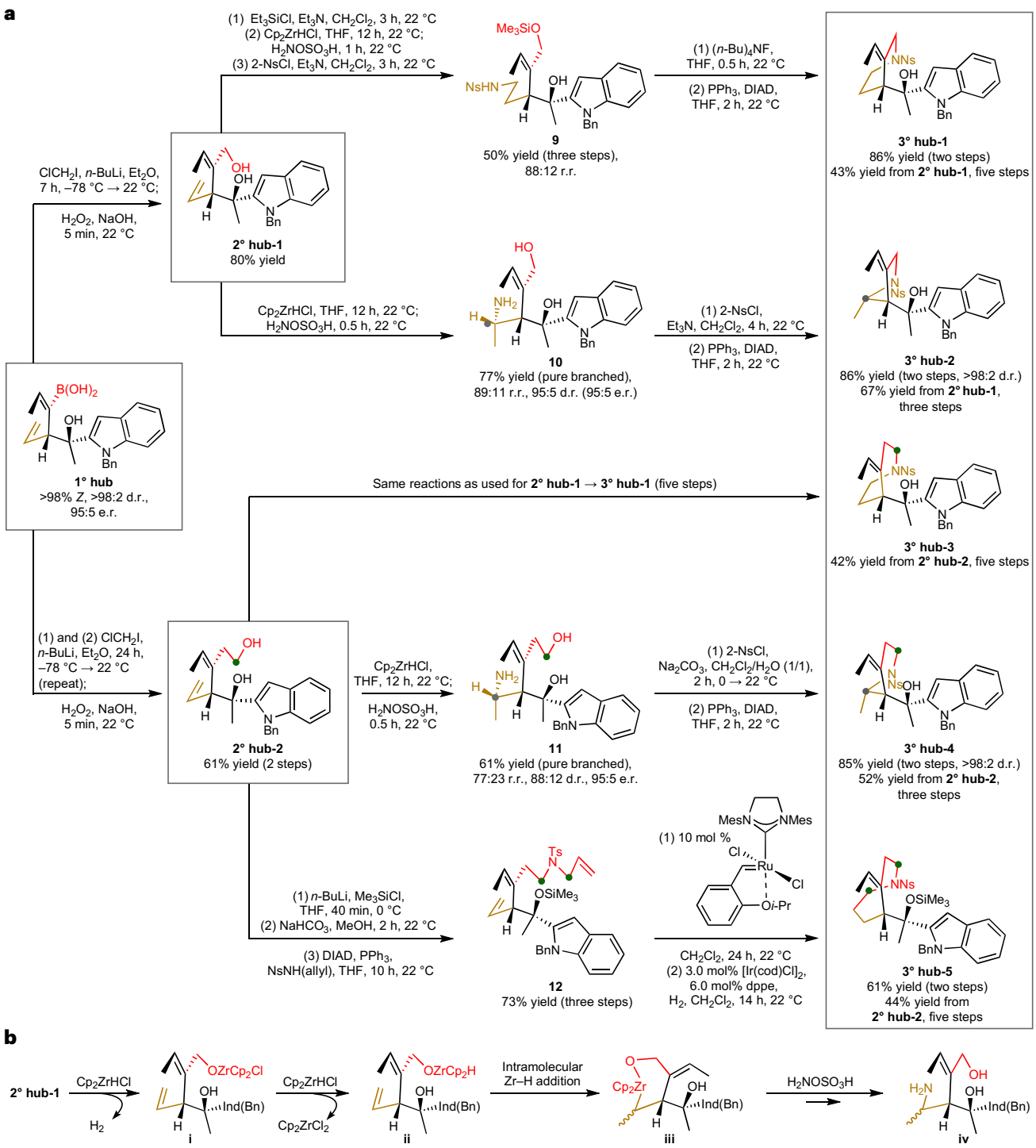

Fig. 4 | Progressively divergent conversion of the primary hub to secondary and tertiary hubs. a, The **1° hub**, containing two key modifiable moieties (alkenyl boronate in red; vinyl unit in brown) was converted to two **2° hubs**, one an allylic and the other a homoallylic alcohol. The **2° hub-1** was then transformed to various tertiary hubs. The **3° hub-1** pertains to the natural framework, and **3° hub-2** is a contracted ring; **2° hub-2** was similarly converted to **3° hub-3** and **3° hub-4**. The **3° hub-5** was generated by a five-step route that included a catalytic ring-closing metathesis and hydrogenation step. **b**, Hydroxy-assisted regioselective hydroamination, affording the α-secondary NH_2-amine product, may be used for contraction of the bridged bicyclic amine. Ns, 2-nitrobenzenesulfonyl; Cp, cyclopentadiene; cod, cyclooctadiene; dppe, 1,2-bis(diphenylphosphino)ethane; Mes, mesityl or 2,4,6-trimethylphenyl; Ind(Bn), benzyl-protected indole. See Supplementary Sections 7 and 8 for details.

hydride (Cp_2ZrHCl) followed by hydroxylamine-*O*-sulfonic acid (HAS). This led to the corresponding α-primary NH_2-amine[34], which was converted to sulfonamide **9** (50% yield for three steps). Unmasking of the primary alcohol set the stage for the first cyclization, which furnished **3° hub-1** (86% yield for two steps).

The ensuing single methylene contraction (see **contracted**, Fig. 1b) proved to be more complicated. The common approach for one-carbon excision, oxidative cleavage of the mono-substituted alkene, was out of the question because of the presence of an indole, an amine and a C–B bond. We reasoned that a possible approach might

https://doi.org/10.1038/s41557-024-01455-7

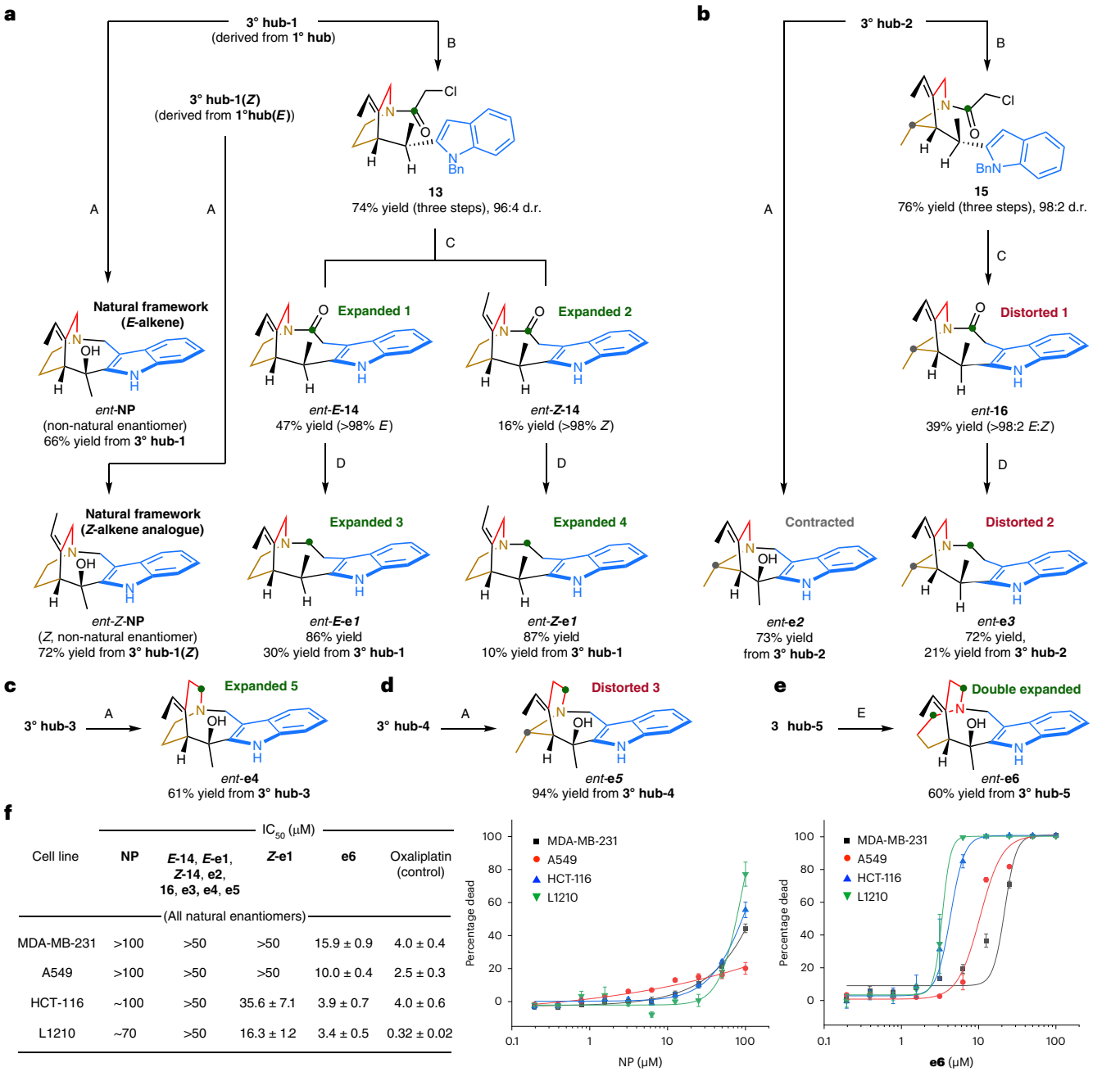

Fig. 5 | Synthesis of the NP and precisely altered scaffolds and in vitro testing. **a**, The **NP** and *Z*-**NP** were obtained in two steps from **3° hub-1**, as was α-chloroamide **13**, the precursor to four expanded scaffolds. **b**, It took seven steps to transform 3° **hub**-2 to a contracted scaffold (*ent*-**e2**) and two distorted scaffolds (*ent*-**16** and *ent*-**e3**). **c**–**e**, 3° **hub**-**3**–3° **hub5** were converted to expanded (*ent*-**e4**) (**c**), distorted (*ent*-**e5**) (**d**) and doubly expanded (*ent*-**e6**) (**e**) frameworks. Green dot denotes an added methylene and grey dot denotes a deleted methylene. Alterations derived from the indolyl moiety are in blue, alterations derived from the alkenyl boronate are in red and alterations derived from the vinyl unit are in brown. **f**, Cytotoxicity (72 h IC_{50} values, μM) against four cancer cell lines (Alamar Blue assay, $n = 3$ biological replicates, error is standard error of the mean (s.e.m.)) underscores the importance of having access to precisely altered skeletal analogues. Oxaliplatin was used as a quantitative dead control. ***Z*-e1** caused some cell death in two of the cell lines, while **e6** exhibited activity for all four cell lines. Condition A: (1) Na/NH_3, THF, 1 h, −78 °C; (2) PPTs, HCHO, THF, 24 h, 22 °C. A′: same as A, except step 2 in DMF. Condition B: (1) TFA, CH_2Cl_2, 2 h, 22 °C; (2) Na/NH_3, *t*-BuOH, 1 h, −78 °C; (3) $ClCH_2COCl$, Et_3N, 1 h, 22 °C. Condition C: *hν* (254 nm), Na_2CO_3, $EtOH/H_2O$, 15 min. Condition D: $LiAlH_4$, THF, 5 h, 60 °C. Condition E: (1) $(n\text{-}Bu)_4NF$, THF, 0.5 h, 22 °C; (2) Na/NH_3, THF, 1 h, −78 °C; (3) PPTs, HCHO, MeCN, 24 h, 22 °C. See Supplementary Sections 9 and 12 for details. *ent*, non-natural isomer; e, edited scaffold; TFA, trifluoroacetic acid; PPTs, pyridinium *p*-toluenesulfonate; MDA-MB-231, human breast cancer cell line; A549, adenocarcinomic human alveolar basal epithelial cell line; HCT-116, human colon cancer cell line; L1210, mouse lymphocytic leukaemia cell line; IC_{50}, half-maximal inhibitory concentration.

entail direct formation of a C–N bond at the internal carbon of the mono-substituted olefin, and use of the resulting secondary amine for cyclization. Ideally, this would be accomplished by a hydroamination that would proceed with the complementary regioselectivity. However, such a method, particularly challenging with a mono-substituted aliphatic olefin substrate[35,36], is yet to be developed. We instead entertained a different option.

In the foregoing synthesis of **3° hub-1**, hydroamination of a mono-substituted alkene (see **2° hub-1** → **3° hub-1**) was carried out by sequential treatment with Cp_2ZrHCl and HAS. We surmised that if

the same were to be performed with an unmasked primary alcohol, an alkoxyzirconocene hydride might be generated first (**2° hub-1** → **i** → **ii**; Fig. 4b). Ensuing intramolecular zirconocene–hydride addition via a more favourable six-membered zirconacycle (**ii** → **iii**)[37,38], and trapping of the C–Zr bond with HAS, would deliver an α-secondary NH_2-amine (**iv**). In the event, subjection of **2° hub-1** to Cp_2ZrHCl followed by HAS afforded **10** in 77% yield, as a single regioisomer and in 95:5 d.r. (after silica gel chromatography). Sulfonamide formation and cyclization furnished **3° hub-2** (67% yield from **2° hub-1**, three steps).

Our next goal was to convert **2° hub-2** to different tertiary hubs (Fig. 4a) with scaffolds wherein a bridge would be expanded by a single methylene group. The first, **3° hub-3**, was prepared as before (in five steps and 42% yield; see **2° hub-1** → **3° hub-1**). Hydroxy-assisted hydroamination of **2° hub-2** afforded α-secondary NH_2-amine **11** with somewhat lower regio- and diastereoselectivity (77:23 regioisomeric ratio (r.r.) and 88:12 d.r.), probably on account of a more distal coordinating unit (compared with allylic alcohol in **2° hub-1**). We isolated **11** in 61% yield, >98:2 r.r. and 95:5 e.r. (after chromatography) and transformed it to **3° hub-4** by the already mentioned sulfonamide formation/cyclization (52% yield from **2° hub-2**, three steps).

The concluding tertiary hub (**3° hub-5**; Fig. 4a) contained two additional methylenes, one within each of the carbon bridges. We obtained this analogue by masking the alcohols and then selectively deprotecting the less hindered silyl ether, followed by conversion to triene **12** (73% yield, three steps). Ring-closing metathesis and site-selective hydrogenation of the cyclic alkene furnished **3° hub-5** (44% yield from **2° hub-2**, five steps). With five tertiary hubs in hand, we were ready to convert them to **NP** and a collection of precisely modified scaffolds.

Syntheses of NP and altered scaffolds

Synthesis of the natural framework (Fig. 5a) began by removal of the nosyl and benzyl groups in **3° hub-1**. The ensuing Pictet–Spengler process delivered *ent*-**NP** (the non-natural enantiomer; 66% yield). We accessed **NP** by using *ent*-**bisphos-2** (also commercially available) and prepared *ent*-***Z***-**NP** similarly from **3° hub-1(*Z*)** (originating from **1°hub(*E*)**). The same may be applied to every tertiary hub's corresponding *Z* isomer.

Conversion of **3° hub-1** to skeletons with a methylene unit inserted between their nitrogen atom and the indole C3 (see **expanded 1**, Fig. 1b) presented additional challenges. The most effective solution turned out to be Witkop cyclization[39], a photochemical process that, to the best of our knowledge, had not been applied to a substrate bearing a somewhat sensitive tertiary benzylic alcohol. Moreover, ring closure was feasible only without the tertiary hydroxy group (fast decomposition, otherwise). Photolysis of α-chloro-amide **13** (Fig. 5a), obtained in three steps from **3° hub-1** (74% yield, 96:4 d.r.), afforded *ent*-***E***-**14** and *ent*-***Z***-**14** (**expanded 1** and **expanded 2**). Analogues *ent*-***E***-**14** and *ent*-***Z***-**14** (readily separable) contain an amide carbonyl, which is a possible point of H-bonding. Amide reduction furnished the expanded, pericine-like (Fig. 1a), bridged bicyclic amines *ent*-***E***-**e1** and *ent*-***Z***-**e1** (**expanded 3** and **expanded 4**, label in italics signifies analogue containing more than one alteration). While loss of the hydroxy group makes this remodelling less precise, other bioactive members of the alkaloid family, such as pericine (Fig. 1a), apparicine[40] and anti-neuroinflammatory geissoschizoline (Fig. 1a), also lack this unit. Curan (Fig. 1a) carries a similar methyl-substituted stereogenic benzylic carbon. By and large, after a total of eight reactions, **3° hub-1** was transformed not only to **NP**, but also to four skeletally expanded analogues.

We transformed **3° hub-2** to *ent*-**e2** (**contracted**; 73% yield; Fig. 5b) by using the same reactions that converted **3° hub-1** to **NP**. Akin to synthesis of *ent*-***E***-**e1** and *ent*-***Z***-**e1**, **3° hub-2** was converted to α-chloro-amide **15** and then *ent*-**16** (**distorted 1**, 30% yield from **3° hub-2**, four steps), which was reduced to *ent*-**e3** (**distorted 2**, 21% yield from **3° hub-2**, five steps). Nosyl and benzyl group removal and Pictet–Spengler cyclization turned **3° hub-3** into *ent*-**e4** (**expanded 5**; Fig. 5c) and 3° **hub-4** into *ent*-**e5** (**distorted 3**; Fig. 5d) in 61% and 94% yields, respectively. The same protocol, preceded by tertiary alcohol unmasking, delivered *ent*-**e6** (**double expanded**) in 60% yield from **3° hub-5** after three steps (Fig. 5e).

At the end, without needing to re-perform an entire route, we were able to secure seven distinct scaffolds after a total of 49 steps. This constituted an average for steps/scaffold efficiency[18] of seven and steps/analogue economy of four.

In vitro testing

In vitro testing was carried out to determine whether the skeletal alterations lead to compounds that possess distinct bioactivity (Fig. 5f). Phenotypic screening[41] was performed to gauge the cytotoxicity of the NP and analogues (that is, enantiomers of compounds shown in Fig. 5a–e; see Supplementary Section 12 for details) against a panel of four cancer cell lines (with oxaliplatin as the control compound[42]). There was no particular rationale for selecting these four cell lines, nor should this imply that further testing involving other cell lines is not warranted. While the original **NP** is weakly anti-malarial[9], this study was performed because we wanted to see if application of the present strategy can identify leads in other disease areas[43].

In actuality, while **NP** and most altered frameworks did not exert any influence, two expanded frameworks promoted cell death. ***Z***-**e1** displayed appreciable cytotoxicity against two of the cell lines and, more notably, **e6** exhibited cytotoxicity against all four. As shown by the dose–response curves, the double-expanded scaffold of **e6** represents a notable shift in bioactivity. Limited testing of the corresponding unnatural enantiomers, which included *ent*-***Z***-**e1**, did not display any cytotoxicity (»50 μM; Supplementary Section 12.4). This underscores the importance of the catalytic enantioselective process.

The structure–activity relationship (SAR) is optimizable. For example, comparison of the data for **e6** and those for **NP** and **e4**, bearing only one of the two one-methylene expansions in **e6**, implies that **e6**'s effectiveness might be due to combined influence of expansion in two bicyclic amine regions or because of this particular one-methylene enlargement. Conversion of **1° hub** to the analogue containing only the latter expansion and biological testing would be one way of gaining further clarity.

Regarding the puzzling selectivity trends

We encountered several perplexing selectivity profiles during our investigations. Mechanistic appreciation of the origins of these trends would enhance the applicability of the catalytic process. Computational investigations were thus performed.

The first observation was the higher *Z*:*E* ratio for the transformation that involved cyclohexyl-substituted vinylallene (*rac*-**2c**) and generated homoallylic alcohol **3c** through reaction with acetophenone (>98:2 *Z*:*E*; Fig. 2b). In contrast, the *Z*:*E* ratio for transformation of *rac*-**2c** and 2-heptanone to afford **6c** was at the frequently observed range (82:18 *Z*:*E*). DFT studies reveal that the transition state leading to the *Z* isomer of **3c** is more favoured, partly owing to London dispersive attraction[44,45] between the axially oriented C–H bonds of the cyclohexyl moiety and the π-cloud of acetophenone's phenyl group (**ts-3c-bisphos-5-maj**; Fig. 6a). Diminished polarizability and enhanced conformational mobility renders the same interaction less influential with an *n*-alkyl-ketone (for example, formation of **6c**). Another reason for higher *Z* selectivity is the greater steric pressure between B(pin) and cyclohexyl groups in the less preferred **ts-3c-bisphos-5-min** compared with when an *n*-alkyl-allene is used (for example, see **3a** and **3b**). While the phenethyl moiety can be engaged in dispersive attraction in the lower energy transition state, its smaller size renders the alternative pathway more competitive (for further analysis, see Supplementary Section 13.5).

Another unforeseen outcome corresponded to the reaction with *ortho*-methoxyacetophenone affording **3g** more enantioselectively

https://doi.org/10.1038/s41557-024-01455-7

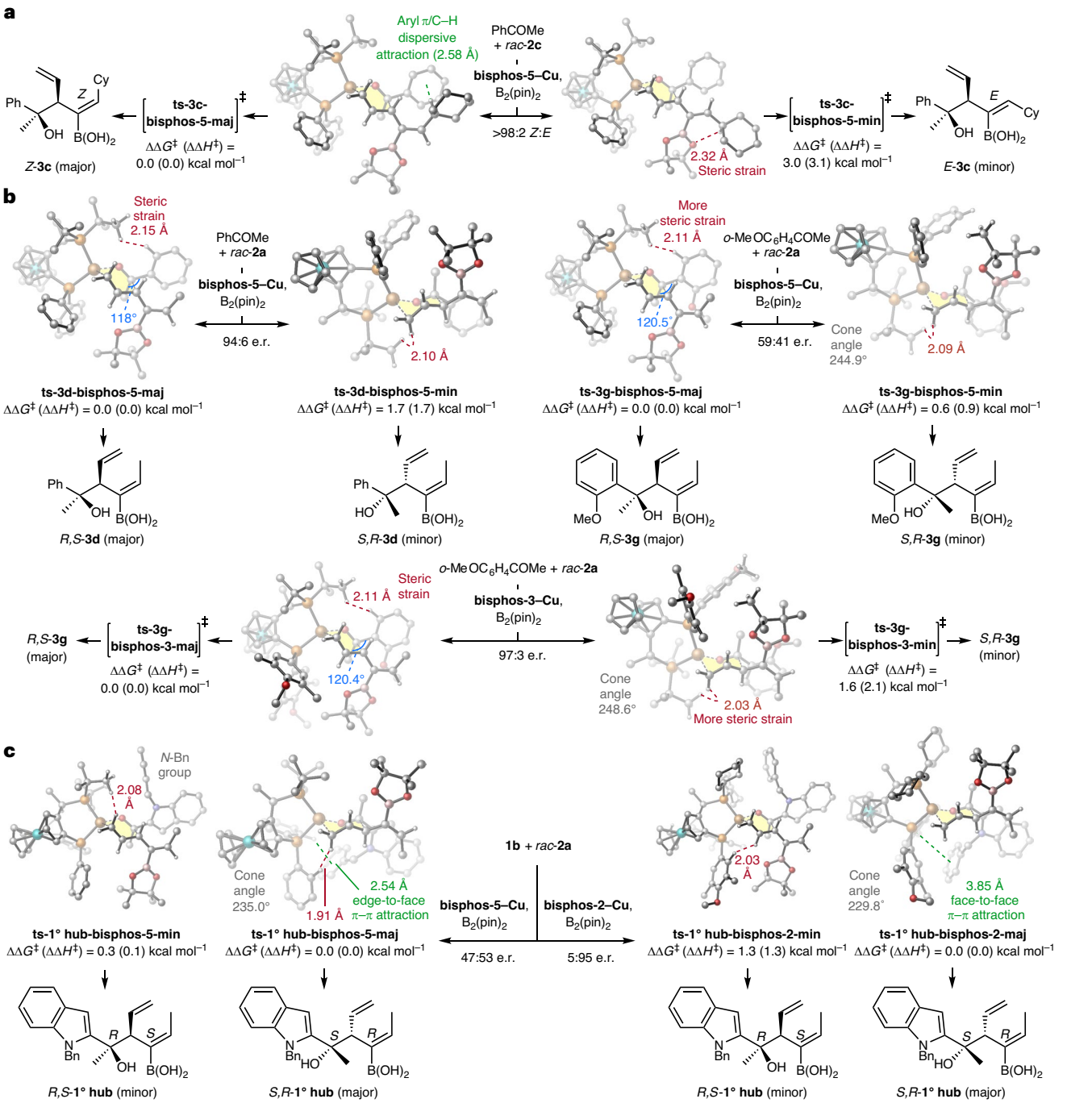

Fig. 6 | DFT studies offer insight regarding several unexpected selectivity trends. a, The higher *Z*:*E* ratio for cyclohexyl-substituted allene may be due to London dispersion attraction between C–H bonds and an aryl group. **b**, For **3g**, the 59:41 e.r. with **bisphos-5** compared with the 97:3 e.r. with **bisphos-3** is probably rooted in conformational differences leading to greater steric strain in **ts-3g-bisphos-5-maj**. With **bisphos-3**, the larger arylphosphine enhances steric pressure in **ts-3g-bisphos-3-min**. **c**, The unexpected low e.r. for **1° hub** formation with **bisphos-5** and enantioselectivity reversal (versus **3d**) with **bisphos-2** was predicted by DFT studies, and appears to be owing to π–π interactions involving the N-benzyl group. The allyl–Cu complex and the ketone associate differently in **ts-1° hub-bisphos-5-maj** (versus **ts-3d-bisphos-5-min**). The difference between **ts-1° hub-bisphos-5** complexes is reduced due to π–π interaction in **ts-1° hub-bisphos-5-maj**. In contrast, steric strain from the proximity of the allyl–Cu and arylphosphine in **ts-1° hub-bisphos-2-min** and a face-to-face attraction in **ts-1° hub-bisphos-2-maj** cause enough energy difference for *S*,*R*-**1° hub** to be formed in 95:5 e.r. DFT studies were performed with M06/SDD-6-311 + G(d,p)/SMD(THF)//B3LYP-D3/SDD-6-31G(d). See Supplementary Section 13 for details.

with **bisphos-3** than the otherwise effective **bisphos-5** (97:3 compared with 59:41, respectively). This discrepancy seems to arise from the larger angle between the aryl and methyl ketone substituents (to minimize allylic strain) in the case of the *ortho*-methoxy variant (120.5° (**ts-3g-bisphos-5-maj**; Fig. 6b) and 118° (**ts-3d-bisphos-5-maj**) for *ortho*-methoxyacetophenone and acetophenone, respectively). Consequently, with **bisphos-5**–**Cu**, the *ortho*-methoxyphenyl moiety is positioned closer to one of the ligand *tert*-butyl groups (2.11 compared with 2.15 Å in **ts-3g-bisphos-5-maj** and **ts-3d-bisphos-5-maj**, respectively). The resulting steric pressure lowers the activation energy difference ($\Delta\Delta G^{\ddagger}$) from 1.7 kcal mol^{-1} for the formation of **3d** to 0.6 kcal mol^{-1}, causing **3g** to be formed with lower e.r. (59:41 compared with 94:6

for **3d**). With **bisphos-3** and its more sizeable triarylphosphine unit, while the preferred addition mode (**ts-3g-bisphos-3-maj**) is impacted nominally (compared with **ts-3g-bisphos-5-maj**), there is an increase in steric repulsion in the transition state for the minor enantiomer (**ts-3g-bisphos-3-min**). This arises from propinquity of the allylic moiety and the catalyst's *tert*-butyl group, engendered by the larger ligand cone angle in **ts-3g-bisphos-3-min** (248.6° compared with 244.9° in **ts-3g-bisphos-5-min**). The gap between the two pathways thus widens to 1.6 kcal mol^{-1}, and **3g** is generated in 97:3 e.r. It follows that the reaction of the ketone with a smaller *ortho*-fluoro-substituted or bicyclic aryl moiety with **bisphos-5** gives homoallylic alcohol **3i** and **3j** in 92:8 e.r., as anticipated.

Just as enigmatic were the data regarding the catalytic multi-component reaction that afforded **1° hub**. With **bisphos-5** the homoallylic alcohol was formed in 53:47 e.r., whereas with **bisphos-2** the multifunctional platform was generated in 95:5 e.r. Equally surprising, but as presaged by DFT studies, the major enantiomer was not the one that we had predicted to be favoured on the basis of the methodological studies (for example, see **3d**; Fig. 2b). There seem to be several reasons for these findings. One is that, with most ketones, their methyl group is situated within the same quadrant as the ligand's arylphosphine and the substrate's aryl or heteroaryl and the *tert*-butyl phosphine moieties reside in a different section (see **ts-3d-bisphos-5-maj**; Fig. 6b). The situation is different with benzyl-protected indolyl ketone **1b**. Here the indolyl fragment preferentially occupies the region that also contains the ligand's arylphosphine (see **ts-1° hub-bisphos-5-maj** and **ts-1° hub-bisphos-2-maj**; Fig. 6c). The reason for this is probably a stabilizing π–π interaction between the N-benzyl group and a phenyl substituent of the catalyst's biarylphosphine moiety (see **ts-1° hub-bisphos-5-maj** (edge-to-face) and **ts-1° hub-bisphos-2-maj** (face-to-face)). The preferred transition state with **bisphos-5**–**Cu**, namely **ts-1° hub-bisphos-5-maj**, although stabilized by a π–π association, suffers from steric repulsion between the allyl moiety and a phenylphosphine (1.91 Å). The net outcome is a negligible energy difference between the two pathways ($\Delta\Delta G^{\ddagger}$ = 0.3 kcal mol^{-1}; 47:53 e.r.). In **ts-1° hub-bisphos-2-maj**, on the other hand, as a consequence of the ligand's smaller cone angle (229.8° compared with 235.0° for **ts-1° hub-bisphos-5-maj**), the abovementioned steric repulsion is ameliorated by an increased distance between copper–allyl and diarylphosphine groups. The energy separation between the competing **bisphos-2**-derived transition states is therefore wider and enantioselectivity higher ($\Delta\Delta G^{\ddagger}$ = 1.3 kcal mol^{-1}; 5:95 e.r.). In the case of N-benzyl-protected indolyl ketone **1b**, a blend of π–π interactions and ligand steric effects cause C–C bond formation to occur preferentially at the ketone enantiotopic face that would otherwise lead to the minor enantiomer.

The DFT-derived rationale is congruent with the lower e.r. for a chiral bisphosphine that has a phosphorus atom attached to two 3,5-bis-trifluoromethylphenyl moieties (instead of a 4-methoxy-3,5-dimethylphenyl groups in **bisphos-2**). In this instance (Fig. 3b), because π–π interaction is weaker with a more electron-deficient arylphosphine, ***S,R***-**1° hub** was generated in 77:23 e.r. (54% yield (pure *Z*), 76:24 *Z*:*E*, >98:2 d.r.; see Supplementary Section 13.8 for details). Further, the reaction involving *N*-2-trimethylsilylethoxymethyl-protected indolyl ketone and **bisphos-2** was less enantioselective (see Supplementary Section 13.9 for details).

Conclusions

We introduce a catalytic regio-, diastereo- and enantioselective multi-component process that was subsequently used in a concise synthesis of an indole alkaloid and several of its precisely altered scaffolds. The catalytically generated **1° hub** was first transformed through a progressively divergent series of 21 reactions, not more than five steps in each stage, to a pair of **2° hubs**. The latter were transformed to five **3° hubs** in high diastereo- and enantiomeric purity. The collection of **3° hubs** was then utilized to access **NP** (11-step LLS, 9.1% overall yield compared with 23-step LLS and 4.7% overall yield, formerly[16]). Ten skeletal analogues were generated after 26 operations. After all was said and done and a total of 49 steps, seven unique scaffolds and 12 different analogues were in hand. This is an average of seven steps per scaffold and four steps per analogue.

The foregoing **2°** and **3° hubs** are only a sample of possible platforms. The alkenyl boronate could, for instance, be subjected to iterative Matteson homologation[46] (instead of mono or double homologation performed here). Alternatively, after a single methylene truncation (hydroxy-assisted hydroamination), the alkenyl boronate might be used for chain extension before cyclization (for example, by catalytic cross-metathesis or hydroformylation) to provide differently expanded scaffolds. The transformations used to obtain the **3° hubs** do not embody an exhaustive list. The multi-component process is not confined to indolyl ketones, and Witkop cyclizations can be performed with **3° hubs-3**–**5**. Many such foci may be converted to skeletally altered analogues of other members of this extensive alkaloid family. The catalytically generated and densely functionalized platforms may be utilized to access other NP types, such as isodactyloxene A[47], charborol B[48], fumagillin[49] and structures represented by TNP-470 (ref. 50).

In vitro studies bring to light the implications of a made-to-order approach to ground-up precise skeletal diversification. The data provided here show that a framework that contains one or two, more or less, methylene units can exhibit an entirely distinct bioactivity profile. Consistent with these expectations, docking studies reveal that different skeletal analogues represent a superior fit for different receptor sites.

Viewed through a wider lens, the findings described here underline the importance of, and the need for, design and development of methods, the applicability of which is not confined to synthesis of NPs. Rather, the ability to secure several precisely altered and unnatural frameworks should also be part of the equation.

Online content

Any methods, additional references, Nature Portfolio reporting summaries, source data, extended data, supplementary information, acknowledgements, peer review information; details of author contributions and competing interests; and statements of data and code availability are available at https://doi.org/10.1038/s41557-024-01455-7.

References

1. Campos, K. R. et al. The importance of synthetic chemistry in the pharmaceutical industry. *Science* **363**, eaat0805 (2019).
2. Grigalunas, M., Burhop, A., Christoforow, A. & Waldmann, H. Pseudo-natural products and natural product-inspired methods in chemical biology and drug discovery. *Curr. Opin. Chem. Biol.* **56**, 111–118 (2020).
3. Guillemard, L., Kaplaneris, N., Ackermann, L. & Johansson, M. J. Late-stage C–H functionalization offers new opportunities in drug discovery. *Nat. Rev. Chem.* **5**, 522–545 (2021).
4. Huigens, R. W. III et al. A ring-distortion strategy to construct stereochemically complex and structurally diverse compounds from natural products. *Nat. Chem.* **5**, 195–202 (2013).
5. Jurczyk, J. et al. Single-atom logic for heterocycle editing. *Nat. Synth.* **1**, 352–364 (2022).
6. McLeod, M. C. et al. Probing chemical space with alkaloid-inspired libraries. *Nat. Chem.* **6**, 133–140 (2014).
7. Fokas, D., Yu, L. & Baldino, C. M. Strategies for the synthesis of indole alkaloid-based screening libraries for drug discovery. *Mol. Divers.* **9**, 81–89 (2005).
8. Shearer, J., Castro, J. L., Lawson, A. D. G., McCoss, M. & Taylor, R. D. Rings in clinical trials and drugs: present and future. *J. Med. Chem.* **65**, 8699–8712 (2022).

9. Noguchi, Y. et al. Synthesis and stereochemical determination of an antiparasitic pseudo-aminal type monoterpene indole alkaloid. *J. Nat. Med.* **70**, 302–317 (2016).
10. Arens, H., Borbe, H. O., Ulbrich, B. & Stöckigt, J. Detection of pericine, a new CNS-active indole alkaloid from *Picralima nitida* cell suspension culture by opiate receptor binding studies. *J. Med. Plant. Res.* **46**, 210–214 (1982).
11. Bonjoch, J., Solé, D., GarcÍa-Rubio, S. & Bosch, J. A general synthetic entry to *strychnos* alkaloids of the curan type via a common 3a-(2-nitrophenyl)hexahydroindol-4-one intermediate. Total syntheses of (±)19,20-dihydroakuammicine, (±)-norfluorocurarine, (±)-echitamidine, and (±)-20-epilochneridine. *J. Am. Chem. Soc.* **119**, 7230–7240 (1997).
12. Michel, S., Tillequin, F. & Koch, M. Brafouédine et isobrafouédine: nouveux alcoïdes indoliques mineurs de strychnos dinklagei. *J. Nat. Prod.* **49**, 452–455 (1986).
13. Lima, J. A. et al. Geissoschizoline, a promising alkaloid for Alzheimer's disease: inhibition of human cholinesterases, anti-inflammatory effects and molecular docking. *Bioorg. Chem.* **104**, 104215 (2020).
14. Arita, T. et al. Discovery of conolidine derivative DS39201083 as a potent novel analgesic without mu opioid agonist activity. *Bioorg. Med. Chem. Lett.* **29**, 1938–1942 (2019).
15. Jhoti, H., Williams, G., Rees, D. C. & Murray, C. W. The 'rule of three' for fragment-based drug discovery: where are we now? *Nat. Rev. Drug Discov.* **12**, 644 (2013).
16. Hirose, T. et al. Structure determination and total synthesis of (+)-16-hydroxy-16,22-dihydroapparicine. *Chem. Eur. J.* **19**, 10741–10750 (2013).
17. Schreiber, S. L. Target-oriented and diversity-oriented organic synthesis in drug discovery. *Science* **287**, 1964–1969 (2000).
18. Galloway, W. R. J. D., Isidro-Llobet, A. & Spring, D. R. Diversity-oriented synthesis as a tool for the discovery of novel biologically active small molecules. *Nat. Commun.* **1**, 80 (2010).
19. Kim, J., Kim, H. & Park, S. B. Privileged structures: efficient chemical 'navigators' toward unexplored biologically relevant chemical spaces. *J. Am. Chem. Soc.* **136**, 14629–14638 (2014).
20. Wilson, R. M. & Danishefsky, S. J. Small molecule natural products in the discovery of therapeutic agents: the synthesis connection. *J. Org. Chem.* **71**, 8329–8351 (2006).
21. Garcia-Castro, M., Zimmermann, S., Sankar, M. G. & Kumar, K. Scaffold diversity synthesis and its application in probe and drug discovery. *Angew. Chem. Int. Ed.* **55**, 7586–7605 (2016).
22. Lusi, R. F., Perea, M. A. & Sarpong, R. C–C bond cleavage of α-pinene derivatives prepared from carvone as a general strategy for complex molecule synthesis. *Acc. Chem. Res.* **55**, 746–758 (2022).
23. Liu, Y.-L. & Lin, X.-T. Recent advances in catalytic asymmetric synthesis of tertiary alcohols via nucleophilic addition to ketones. *Adv. Synth. Catal.* **361**, 876–918 (2019).
24. Meng, F., Jang, H., Jung, B. & Hoveyda, A. H. Cu-catalyzed chemoselective preparation of 2-(pinacolato)boron-substituted allylcopper complexes and their in situ site-, diastereo- and enantioselective additions to aldehydes and ketones. *Angew. Chem. Int. Ed.* **52**, 5046–5051 (2013).
25. Tsai, E. Y., Liu, R. Y., Yang, Y. & Buchwald, S. L. A regio- and enantioselective CuH-catalyzed ketone allylation with terminal allenes. *J. Am. Chem. Soc.* **140**, 2007–2011 (2018).
26. Yang, Y., Perry, I. B., Lu, G., Liu, P. & Buchwald, S. L. Copper-catalyzed asymmetric addition of olefin-derived nucleophiles to ketones. *Science* **353**, 144–150 (2016).
27. Li, C. et al. CuH-catalyzed enantioselective ketone allylation with 1,3-dienes: scope, mechanism, and applications. *J. Am. Chem. Soc.* **141**, 5062–5070 (2019).
28. Feng, J.-J., Xu, Y. & Oestreich, M. Ligand-controlled diastereodivergent, enantio- and regioselective copper-catalyzed hydroxyalkylboration of 1,3-dienes with ketones. *Chem. Sci.* **10**, 9679–9683 (2019).
29. Fu, B. et al. Copper-catalyzed asymmetric reductive allylation of ketones with 1,3-dienes. *Org. Lett.* **21**, 3576–3580 (2019).
30. Huang, Y., Torker, S., Li, X., del Pozo, J. & Hoveyda, A. H. Racemic vinylallenes in catalytic enantioselective multicomponent processes: rapid generation of complexity through 1,6-conjugate additions. *Angew. Chem. Int. Ed.* **58**, 2685–2691 (2019).
31. Matteson, D. S. & Sadhu, K. M. Boronic ester homologation with 99% chiral selectivity and its use in syntheses of the insect pheromones (3*S*,4*S*)-4-methyl-3-heptanol and *exo*-brevicomin. *J. Am. Chem. Soc.* **105**, 2077–2078 (1983).
32. Hoveyda, A. H., Hird, A. W. & Kacprzynski, M. A. Small peptides as ligands for catalytic asymmetric alkylations of olefins. Rational design of catalysts or of searches that lead to them? *Chem. Commun.* **21**, 1779–1785 (2004).
33. Blakemore, P. R. & Burge, M. S. Iterative stereospecific reagent-controlled homologation of pinacol boronates by enantioenriched α-chloroalkyllithium reagents. *J. Am. Chem. Soc.* **129**, 3068–3069 (2007).
34. Strom, A. E. & Hartwig, J. F. One-pot anti-Markovnikov hydroamination of unactivated alkenes by hydrozirconation and amination. *J. Org. Chem.* **78**, 8909–8914 (2013).
35. Bernoud, E. et al. Recent advances in metal free-and late transition metal-catalysed hydroamination of unactivated alkenes. *Catal. Sci. Technol.* **5**, 2017–2037 (2015).
36. Huang, L. et al. Late transition metal-catalyzed hydroamination and hydroamidation. *Chem. Rev.* **115**, 2596–2697 (2015).
37. Takaya, H., Yamakawa, M. & Mashima, K. Synthesis and characterization of 2-[di(cyclopentadienyl)zircona]-1-oxacyclopentanes. X-ray crystal structure of $[(\eta\text{-}C_5H_5)_2ZrOCH_2CH_2CHMe]_2$. *J. Chem. Soc. Chem. Commun*. 1283–1284 (1983).
38. Liu, X. & Ready, J. M. Directed hydrozirconation of homopropargylic alcohols. *Tetrahedron* **64**, 6955–6960 (2008).
39. Gritsch, P. J., Leitner, C., Pfaffenbach, M. & Gaich, T. The Witkop cyclization: a photoinduced C–H activation of the indole system. *Angew. Chem. Int. Ed.* **53**, 1208–1217 (2014).
40. Joule, J. A. et al. Alkaloid studies. Part XLVIII. The structure of apparicine, a novel aspidosperma alkaloid. *J. Chem. Soc.* **87**, 4773–4780 (1965).
41. Moffat, J. G., Vincent, F., Lee, J. A., Eder, J. & Prunotto, M. Opportunities and challenges in phenotypic drug discovery: an industry perspective. *Nat. Rev. Drug Discov.* **16**, 531–543 (2017).
42. Ghanbarian, M., Afgar, A., Yadegarazari, R., Najafi, R. & Teimoori-Tolabi, L. Through oxaliplatin resistance induction in colorectal cancer cells, increasing ABCB1 level accompanies decreasing level of miR-302c-5p, miR-3664-5p and miR-129-5p. *Biomed. Pharmacol.* **108**, 1070–1080 (2018).
43. Kobayashi, J. et al. Subincanadines A–C, novel quaternary indole alkaloids from *Aspidosperma subincanum*. *J. Org. Chem.* **67**, 6449–6455 (2002).
44. Fujii, A. et al. Experimental and theoretical determination of the accurate CH/π interaction energies in benzene–alkane clusters: correlation between interaction energy and polarizability. *Phys. Chem. Chem. Phys.* **13**, 14131–14141 (2011).
45. Wagner, J. P. & Schreiner, P. R. London dispersion in molecular chemistry—reconsidering steric effects. *Angew. Chem. Int. Ed.* **54**, 12274–12296 (2015).
46. Burns et al. Assembly-line synthesis of organic molecules with tailored shapes. *Nature* **513**, 183–188 (2014).

47. Ji, N.-Y. et al. Diterpenes, sesquiterpenes, and a C_{15}-acetogenin from the marine red alga *Laurencia mariannenins*. *J. Nat. Prod.* **70**, 1901–1905 (2007).
48. Zhang, W.-H., Williams, I. D. & Che, C.-T. Chabrolols A, B, and C, three new norditerpenes from the soft coral *Nephthea charbroli*. *Tetrahedron Lett.* **42**, 4681–4685 (2001).
49. Sin, N. et al. The anti-angiogenic agent fumagillin covalently binds and inhibits the methionine aminopeptidase, MetAP-2. *Proc. Natl Acad. Sci. USA* **94**, 6099–6103 (1997).
50. Lu, J., Chong, C. R., Hu, X. & Liu, J. O. Fumarranol, a rearranged fumagillin analogue that inhibits angiogenesis in vivo. *J. Med. Chem.* **49**, 5645–5648 (2006).

Reporting summary
Further information on research design is available in the Nature Portfolio Reporting Summary linked to this article.

Data availability
All data in support of the findings of this study are available within the article and its Supplementary Information. Crystallographic data for the structures reported in this article have been deposited at the Cambridge Crystallographic Data Centre, under deposition numbers CCDC 2237819 (**7b**) and 1874716 (**8**). Source data are provided with this paper.

Acknowledgements
The methodological aspects of this work were funded by the NIH (grant R35 GM-130395 to A.H.H.). Support for applications to synthesis of **NP** and the corresponding analogues was provided by the CNRS, the ANR (project PRACTACAL to A.H.H.), the Jean-Marie Lehn Foundation for Chemistry Research (University of Strasbourg, to A.H.H.) and the Circle Gutenberg Foundation (2020 Chair for A.H.H.). Additional support was provided by the University of Illinois (for P.J.H.) and the NIH (grant R35 GM-128779 to P.L.). We thank the Shanghai Institute of Organic Chemistry and Solvay, S.A. for a postdoctoral and a predoctoral fellowship to Y.H. and X.L., respectively. In vitro testing was performed at the University of Illinois, Urbana-Champain. DFT and PMI studies were carried out at the Center for Research Computing at the University of Pittsburgh, Bridges 2 supercomputer at the San Diego Supercomputer Center through allocation TG-CHE140139 from the Advanced Cyberinfrastructure Ecosystem: Services and Support (ACCESS) programme, funded by NSF grants. We are grateful to F. Romiti, M. Formica, S. Ng, S. Xu and A. Nikbakht for helpful discussions.

Author contributions
A.H.H., X.L. and Y.H. designed and developed the catalytic multi-component method and prepared the natural products and skeletal analogues. P.J.H., E.J.T. and A.J.S. performed the in vitro testing. P.L. and B.K.M. designed and performed the DFT studies. A.H.H. conceived the project, directed the investigations and wrote the paper, and the other authors provided editorial advice.

Competing interests
The authors declare no competing interests.

Additional information
Supplementary information The online version contains supplementary material available at https://doi.org/10.1038/s41557-024-01455-7.

Correspondence and requests for materials should be addressed to Paul J. Hergenrother, Peng Liu or Amir H. Hoveyda.

Peer review information *Nature Chemistry* thanks Kevin Kou and the other, anonymous, reviewer(s) for their contribution to the peer review of this work.

nature portfolio

Corresponding author(s): Amir H. Hoveyda, Peng Liu and Paul J. Hergenrother

Last updated by author(s): Nov 30, 2023

Reporting Summary

Nature Portfolio wishes to improve the reproducibility of the work that we publish. This form provides structure for consistency and transparency in reporting. For further information on Nature Portfolio policies, see our Editorial Policies and the Editorial Policy Checklist.

Statistics

For all statistical analyses, confirm that the following items are present in the figure legend, table legend, main text, or Methods section.

n/a	Confirmed
☒	☐ The exact sample size (*n*) for each experimental group/condition, given as a discrete number and unit of measurement
☒	☐ A statement on whether measurements were taken from distinct samples or whether the same sample was measured repeatedly
☒	☐ The statistical test(s) used AND whether they are one- or two-sided *Only common tests should be described solely by name; describe more complex techniques in the Methods section.*
☒	☐ A description of all covariates tested
☒	☐ A description of any assumptions or corrections, such as tests of normality and adjustment for multiple comparisons
☒	☐ A full description of the statistical parameters including central tendency (e.g. means) or other basic estimates (e.g. regression coefficient) AND variation (e.g. standard deviation) or associated estimates of uncertainty (e.g. confidence intervals)
☒	☐ For null hypothesis testing, the test statistic (e.g. *F*, *t*, *r*) with confidence intervals, effect sizes, degrees of freedom and *P* value noted *Give P values as exact values whenever suitable.*
☒	☐ For Bayesian analysis, information on the choice of priors and Markov chain Monte Carlo settings
☒	☐ For hierarchical and complex designs, identification of the appropriate level for tests and full reporting of outcomes
☒	☐ Estimates of effect sizes (e.g. Cohen's *d*, Pearson's *r*), indicating how they were calculated

Our web collection on statistics for biologists contains articles on many of the points above.

Software and code

Policy information about availability of computer code

Data collection	N/A
Data analysis	N/A

For manuscripts utilizing custom algorithms or software that are central to the research but not yet described in published literature, software must be made available to editors and reviewers. We strongly encourage code deposition in a community repository (e.g. GitHub). See the Nature Portfolio guidelines for submitting code & software for further information.

Data

Policy information about availability of data

All manuscripts must include a data availability statement. This statement should provide the following information, where applicable:

- Accession codes, unique identifiers, or web links for publicly available datasets
- A description of any restrictions on data availability
- For clinical datasets or third party data, please ensure that the statement adheres to our policy

All data in support of the findings of this study are available within the Article and its Supplementary Information. Crystallographic data for the structures reported in this Article have been deposited at the Cambridge Crystallographic Data Centre, under deposition numbers CCDC 2237819 and 1874716.

Research involving human participants, their data, or biological material

Policy information about studies with human participants or human data. See also policy information about sex, gender (identity/presentation), and sexual orientation and race, ethnicity and racism.

Reporting on sex and gender	N/A
Reporting on race, ethnicity, or other socially relevant groupings	N/A
Population characteristics	N/A
Recruitment	N/A
Ethics oversight	N/A

Note that full information on the approval of the study protocol must also be provided in the manuscript.

Field-specific reporting

Please select the one below that is the best fit for your research. If you are not sure, read the appropriate sections before making your selection.

☒ Life sciences ☐ Behavioural & social sciences ☐ Ecological, evolutionary & environmental sciences

For a reference copy of the document with all sections, see nature.com/documents/nr-reporting-summary-flat.pdf

Life sciences study design

All studies must disclose on these points even when the disclosure is negative.

Sample size	No statistical methods were used to predetermine sample sizes.
Data exclusions	No data were excluded from the analyses.
Replication	Three biological (independent) replications, as indicated in the manuscript, were performed for IC50 determination.
Randomization	Randomization was not relevant for this study.
Blinding	Investigators were not blinded.

Reporting for specific materials, systems and methods

We require information from authors about some types of materials, experimental systems and methods used in many studies. Here, indicate whether each material, system or method listed is relevant to your study. If you are not sure if a list item applies to your research, read the appropriate section before selecting a response.

Materials & experimental systems

n/a	Involved in the study
☒	☐ Antibodies
☐	☒ Eukaryotic cell lines
☒	☐ Palaeontology and archaeology
☒	☐ Animals and other organisms
☒	☐ Clinical data
☒	☐ Dual use research of concern
☒	☐ Plants

Methods

n/a	Involved in the study
☒	☐ ChIP-seq
☒	☐ Flow cytometry
☒	☐ MRI-based neuroimaging

Eukaryotic cell lines

Policy information about cell lines and Sex and Gender in Research

Cell line source(s)	Cells were obtained from ATCC. A549 (Human lung cancer), MDA-MB-231 (Human breast cancer) and HCT-116 (Human colon cancer) were grown in RPMI (Roswell Park Memorial Institute Medium) with 10% fetal bovine serum (GeminiBio). L1210

	(Mouse lymphocytic leukemia) was grown in DMEM (Dulbecco's minimal essential medium) with 10% horse serum (Gibco).
Authentication	Cell lines were authenticated by a commercial vendor and inspected visually in house.
Mycoplasma contamination	The cells were not tested for mycoplasma contamination.
Commonly misidentified lines (See ICLAC register)	No commonly misidentified cell lines were used.

Plants

Seed stocks	N/A
Novel plant genotypes	N/A
Authentication	N/A